IV–10. Seismic Behavior of Brick Masonry Piers

P.A. Hidalgo
Visiting Associate Research Engineer, Earthquake Engineering Research Center (EERC), Univ. of California, Berkeley, Ca.

R.L. Mayes
Assistant Research Engineer, EERC Univ. of California, Berkeley, Ca. and Principal Computech, Berkeley, Ca.

H.D. McNiven
Professor of Engineering Science, Univ. of California, Berkeley, Ca.

R.W. Clough
Professor of Civil Engineering and Assistant Director EERC, Univ. of California, Berkeley, Ca.

ABSTRACT

Experiments that have been conducted to evaluate the seismic resistance of window piers typical of high-rise brick masonry construction are described. Forty-six fixed ended piers were subjected to cyclic, in-plane shear loads. Principal test parameters were the type of masonry construction, the height to width ratio, the amount of reinforcement and the effect of full and partial grouting. The paper also includes an identification of the principal modes of failure, the ultimate strength associated with the modes of failure and the effect of the test parameters on the ultimate strength. Also included is a discussion of the methods to predict the strength associated with each of the modes of failure and a discussion of the inelastic characteristics of piers exhibiting the shear mode of failure. In particular, the effects of horizontal reinforcement and partial grouting on the shear mode are presented.

On décrit quarante six essais où on évalue la résistance et le comportement sismique des mures typiques des batiments en hauteur en maconnerie armée. Dans chaque essai, ces élements ont étés soummis à des charges horizontales cycliques dans le plan du mure. Les principaux paramètres ont étés le type de construction utilisé, la relation hauteur/largeur des mures, le renforcement, et le remplissage partiel ou total des cellules.

Parmi les résultats on présente les principales formes de faille observées, les résistances finales et l'effet de la variation des paramètres sur cettes résistances. On fait une discusion des méthodes de prediction de la résistance finale des mures et on analyse les caracteristiques de comportement inelastique des mures qui ont presenté des failles par cisaillement, en tenant compte specialement l'effet de renforcement horizontal et du remplissage des cellules.

Es werden sechsundvierzig Versuche beschrieben dessen Ziel war die Wiederstandsfähigkeit und das seismische Verhalten von typischen Wänden in Stahlverstärkten Ziegelsteinhochbauten zu erfassen.

In den Versuchen wurden die vorhergehend genannten Bauteile, zyklischen, horizontalen, in der Ebene der Wände enthaltenen Kräfte unterworfen.

Die wichtigsten Parameter die in betracht genommen wurden waren die Bauart, der Bruchteil Höhe/Breite der Wände, die Stahlverstärkung und die Füllung aller oder nur einiger der Zellen der Ziegelsteine.

Unter den Ergebnissen die dargestellt werden befinden sich die Bruchtypen die beobachtet wurden, der entsprechende Bruchwiederstand und der Einfluß auf die Bruchlast der verschiedenen Parameter die in betracht genommen wurden.

Es werden Methoden dergestellt um den Bruchwiederstand einschätzen zu konnen und es werden die nichtlinearen Eigenschaften der Wände dessen Bruch durch Scheerkräfte erzeugt wurde, untersucht. Dabei wird der Einfluß der horizontalen Stahlverstärkung und der Grad der Füllung der Zellen der Zeigelsteine ganz besonders in kauf genommen

Si discrivono cuaranta e sei sággi sperimentali destinati a evaluare la resistenza ed il comportamento sísmico di muri típici di edifici alti, di albagnilería armata. I sággi consisteno in sommettere a questi elementi a cargue orizzontali cícliche contenute nel piano del muro. I principali parámetri considerati nelle studio sono stati: el tipo di costruzione utilizata, il quoziénte alto/largo dei muri, la quantitá di riforzo e il ripieno parciale o totali delli celde.

Fra i risultati che si presenteno si includono i principali modi di fallimento che si esservano, la resistenze ultima associata ad ogni uno di loro, ed il efféttо della variazione dei parámetri in quelle resistenze. Si discutono metidi per predire la resistenza ultima dei muri e si analizano le caratteristiche del comportamento inelastico mostrato per i muri che fallirono per lo sforzo di corte, considerando specialmente l' effetto della quantitá del riforzo orizzontale e del ripieno di celde nel menzionato comportamento.

INTRODUCTION

In determining the lateral load capacity of masonry piers and panels, the first step is to identify the mode of failure. Because most failures in past earthquakes have been characterized by diagonal cracks, many research programs have concentrated on this type of failure mechanism. Test techniques used by Blume,[1] Greenley and Cattaneo,[3] and others, induce the diagonal tension on shear mode of failure. Scrivener,[12] Meli,[9] Williams[13] and Priestley and Bridgeman[10] recognized that there are two possible modes of failure for cantilever piers. In addition to the shear or diagonal tension mode of failure, they recognized that for certain piers, a flexural failure could occur. This mechanism is characterized by yielding of the tension steel of the wall, followed by a secondary compressive failure at the toe, with associated buckling of the reinforcement once confinement is lost.

Priestley[11] has performed several extensive series of tests on cantilever piers and has shown that very desirable inelastic behavior can be obtained with the flexural mode of failure. Consistent with this result, he has recommended that in the conceptual design of a building, all walls be designed to act as cantilever walls (Fig. 1) so that desirable inelastic structural behavior is attained. It is clear that this may be a difficult architectural constraint, and consequently the inelastic behavior of walls other than cantilever walls must be investigated.

Mayes and Clough tested seventeen hollow concrete block, double-pier panels.[7] The panels were approximately 15 ft square and consisted of a top and bottom spandrel and two piers separated by a window opening. The advantage of this test specimen was that the piers had realistic fixed-end boundary conditions, as commonly found in many piers in multistory masonry buildings. The double pier tests were devised to investigate the effect of variations in bearing stress and horizontal and vertical reinforcement on the mode of failure and inelastic behavior. These tests showed that the flexural mode of failure in a fixed ended pier had desirable characteristics, however, these were not as desirable as those obtained by Priestley with cantilever piers. Furthermore, it was recognized that the amount of horizontal reinforcement used in Priestley's tests was substantially greater than that required by the current Uniform Building Code (UBC). This fact and the recognition that the flexural mode of failure is difficult to achieve in fixed ended piers with either a low height to width ratio or a significant compressive force, led to an investigation on the effects of lesser amounts of horizontal reinforcement on the shear mode of failure.

The cost of the double pier tests, both in money and time, precluded carrying out the rest of the test program using this test procedure, and consequently, the single pier test setup shown in Fig. 2 was developed. The forty-six single pier tests reported herein are part of a total of eighty tests. Table 1 shows the number of specimens and parameters varied during the forty-six single pier tests. The overall dimensions of the single piers varied from 80 in. high and 42 in. wide for the specimens with height to width ratio of 2 (HCBR-21 and CBRC-21), to 56 in. high and 48 in. wide for the specimens with height to width ratio of 1 (HCBR-11 and CBRC-11), to 40 in. high and 78 in. wide for the specimens with height to width ratio of 0.5 (HCBR-12 and CBRC-12). The hollow clay brick piers (HCBR) were constructed from standard two-core reinforceable hollow clay bricks, nominally 8 in. wide by 4 in. high by 12 in. long. The double wythe grouted core clay brick piers (CBRC) were constructed from two wythes of clay brick units nominally 4 in. wide by 4 in. high by 12 in. long; the grouted core between the two wythes was nominally 2 in. thick giving the test specimens a thickness of 10 in. All the details of the tests are given in Refs. 2, 4 and 5.

The test equipment, shown in Fig. 2, permits lateral loads to be applied in the plane of the piers using displacement controlled actuators with a maximum capacity of 450 kip. A vertical load may be applied to the piers through the springs and rollers shown above the lateral loading beam in Fig. 2. All the single pier tests had an initial bearing stress of 50 psi. The lateral loading sequence for each test consisted of sets of three sinusoidal displacement cycles applied at a specified actuator displacement amplitude. The specified amplitude was gradually increased and followed a sequence that varied according to the height to width ratio of the piers. The cyclic frequency was maintained at 0.02 Hz.

In the single pier test setup (Fig. 2), the two hinged external steel columns restrain the rotation of the top of the pier, forcing it towards a condition of rotation fixity at the top and bottom, similar to that of the top and bottom spandrel in the double pier test setup.[7] The disadvantage of this test procedure is that the vertical load acting on the pier could not be controlled during the test, and in fact, increased as the in-plane horizontal displacement of the test specimen increased. Consequently, all of the single piers had a significant compressive load acting with the shear cracking load, as reported in Table 1.

TEST RESULTS

The basic product obtained from the tests was the hysteresis loops diagram, which is a plot of the lateral load against the lateral displacement of the piers. The strength and deformation properties, the stiffness degradation and the energy dissipation characteristics of the piers can be obtained from the hysteresis loops.

The test results include the envelopes of the hysteresis loops for most tests (Figs. 3 to 5). The hysteresis envelopes are a plot of the absolute average of the maximum positive and negative forces and corresponding displacements, for each of the three cycles of loading at a given input displacement amplitude. Table 1 includes listings of the maximum shear forces (and stresses) and the axial force (and stresses) present in the pier at the time the maximum shear force was attained. The peak ultimate value is the maximum shear force obtained in any one cycle of loading. The average ultimate value is the maximum value obtained from the hysteresis envelope. This is always less than the peak value, but except for a few cases, it is within 90 percent of the peak value. Table 1 also includes the values for the shear crack strength and the associate compressive stresses. The shear crack strength is the lateral

load required to develop the first major diagonal crack in the pier.

In evaluating the inelastic characteristics of the pier behavior, the hysteresis envelopes provide a good visual picture, however, they must be considered in conjunction with other results to fully evaluate the inelastic behavior. The other results include the energy dissipated per cycle, the ultimate strength, indicators of ductility, and comparisons of crack patterns at equal displacements. The usefulness of hysteresis envelopes is that they provide visual comparisons of ductility and ultimate strength; however, they give no indication of the energy dissipated per cycle. The hysteresis envelopes (average maximum force-deflection curves) are used as a frame of reference for the discussion of the test results. The question as to what constitutes desirable inelastic behavior has been discussed in reference[7] pp. 68–70 in qualitative terms.

DISCUSSION OF THE TEST RESULTS

The discussion of the test results is presented in two sections; the first on the modes of failures observed and the prediction of the ultimate strength, and the second on the inelastic characteristics of the pier behavior.

Modes of Failure and Prediction of Ultimate Strength

Almost all the piers exhibited a shear mode of failure. This mode was characterized by early flexural cracks at the toes of the pier which were later augmented by diagonal cracks that extended through a partial zone of the pier. As the horizontal load increased, large diagonal cracks (x-cracks) formed when the diagonal tensile stress in the pier reached the tensile strength capacity of the masonry. Nine of the piers with height to width ratio of 2 and nine of the piers with height to width ratio of 1, all fully grouted, exhibited yielding in the vertical reinforcement before the occurrence of the major diagonal cracks. However, as the vertical compressive load induced by the single pier test setup increased, the flexural moment capacity of the pier sections also increased while the tension vertical reinforcement continued to yield. This effect allowed the lateral load on the pier to increase until the diagonal tensile stress reached the tensile strength of the masonry and a shear failure developed.

Eight of the piers with a height to width ratio of 0.5 developed a sliding mode of failure along paths determined by previous cracks. In five of the piers sliding occurred along the bottom section of the pier and was prompted by flexural cracks developed along that section. In the other three piers, the final failure mechanism included a combination of shear cracks and sliding along a path determined by these diagonal cracks and the top section of the pier (a bell-shape path). In most of the piers exhibiting a sliding mechanism of failure, major diagonal cracks had developed before the final failure was attained.

The "shear lateral load capacity" (lateral load capacity associated with the shear mode of failure) may be defined at two levels. The "shear crack strength" is defined as the lateral load required to produce the first major diagonal crack; the "ultimate shear strength" is the maximum lateral load developed by the piers. In the case of the piers with height to width ratios of 2 or 1, both quantities are the same (Table 1). In the case of the squat piers (height to width ratio of 0.5), the lateral load continued to increase after the occurrence of the first major diagonal crack because the compression toe of the pier was wide enough to carry a significant shear. Increased amounts of cracking finally produced the failure of the pier at ultimate loads that exceeded the shear crack strength by percentages varying from 5% (CBRC piers), to 11% (HCBR piers) (Table 1).

Concurrent with the erection of the fully grouted piers, prisms and square panels were constructed using the same mortar, grout and masonry units. The prisms were one brick wide, had the same thickness as the piers and a height five times the thickness. The square panels had the same thickness as the piers and the panel dimension was 36 in. The prisms were tested in uniaxial compression and the panels in diagonal compression.[8] These were performed during tests of corresponding piers. Table 2 presents the results of the prism compressive strengths f'_m, the panel critical tensile strengths σ°_{tcr} as formulated by Blume,[1] the pier strength associated with the occurrence of the first major diagonal crack τ_s, and the pier critical tensile strength σ_{tcr}. The pier critical tensile stress was computed at the neutral axis of the pier sections, following the simple beam theory for a section under combined flexure, shear and axial force; a parabolic distribution of shear stresses over the cross section was assumed.[6] In addition to these values, Table 2 also presents the ratios $\sigma^\circ_{tcr}/\sigma^\circ_{tcr}$ and $\tau_s/\sqrt{f'_m}$ for all tests. These ratios illustrate a trend towards an increase in the shear crack strength as both the amount of horizontal reinforcement and the axial compressive stress increase. It is also important to note that these effects on the shear crack strength of the piers are better reflected by the prism strength $\sqrt{f'_m}$ than by the critical tensile strength σ°_{tcr} of the square panels. This is somewhat surprising in that the square panel test is considered to be more sophisticated than the prism test since it induces a diagonal tension failure similar to that observed in the piers.

Inelastic Behavior of Piers

The inelastic characteristics of piers exhibiting a shear mode of failure are discussed in connection with two of the parameters used in the test program: the amount of horizontal reinforcement and the type of grouting. In addition to these two variables, it is important to report that more desirable inelastic behavior was obtained with the more squat piers when compared to the behavior of the piers with height to width ratio of 2 or 1 (Figs. 3 and 4).

In general, horizontal reinforcement has a positive effect on the inelastic behavior of the hollow clay brick piers (Fig. 3). Increasing amounts of horizontal reinforcement improve crack patterns, increase the ultimate strength of the piers and increase their deformation capacity. However, there is not a consistent relationship between the amount of reinforcement and the degree of improvement obtained. Increasing amounts of horizontal

reinforcement has no effect on the rate of strength degradaton of the piers after the ultimate strength has been attained. For the double wythe, grouted core, clay brick piers horizontal reinforcement has little or no influence on the inelastic behavior (Fig. 4).

With respect to the influence of the type of grouting, fully grouted HCBR piers definitively have more desirable inelastic behavior than the corresponding partially grouted piers. The deformation capability of the partially grouted HCBR piers is reduced, the strength degradation becomes very sharp and the ultimate strength based on net area stresses is always less than that of the corresponding fully grouted piers (Fig. 5).

SUMMARY OF TEST RESULTS

1. The strength associated with the shear mode of failure is a function of the tensile strength of the masonry assemblage and is affected by the axial stress on the pier and the amount of horizontal reinforcement. Two methods were used to predict the shear strength of the piers; the method currently used in the Uniform Building Code gives more consistent results.
2. The inelastic behavior characteristics of the shear mode of failure are generally brittle and, except for the piers with height to width ratio of 0.5, the serviceability of the piers is lost with the formation of the first major diagonal shear crack.
3. The inelastic behavior of hollow clay brick piers exhibiting a shear mode of failure is marginally improved with the use of horizontal reinforcement, whereas for the double wythe, grouted core, clay brick piers there is little or no improvement. Fully grouted piers have significantly more desirable inelastic behavior when compared to corresponding partially grouted hollow clay brick piers.

ACKNOWLEDGEMENTS

The research reported in this paper has been jointly funded by the National Science Foundation, the Masonry Institute of America and the Western States Clay Products Association. The sponsorship of these institutions is gratefully acknowledged. Many helpful suggestions have been made by members of the masonry industry, including Messrs. W. Dickey, J. Amrhein, L. Thompson, D. Wakefield, J. Tawresey, S. Beavers, D. Prebble and other members of technical committees of various masonry organizations. D.A. Sullivan Co. fabricated the pier specimens. Thanks are also due to the EERC Laboratory Staff headed by D. Steere and I. Van Asten.

REFERENCES

1. Blume, J.A. and Proulx, J., "Shear in Grouted Brick Masonry Wall Elements," Report to Western States Clay Products from J.A. Blume and Associates, 1968.
2. Chen, S-W.J., Hidalgo, P.A., Mayes, R.L., Clough, R.W., and McNiven, H.D., "Cyclic Loading Tests of Masonry Single Piers, Volume 2—Height to Width Ratio of 1," Report No. UCB/EERC-78/28, University of California, Berkeley, 1978.
3. Greenley, D.G. and Cattaneo, L.E., "The Effect of Edge Load on the Racking Strength of Clay Masonry," Proceedings, Second International Brick Masonry Conference, Stoke-on-Trent, 1970.
4. Hidalgo, P.A., Mayes, R.L., McNiven, H.D. and Clough, R.W., "Cyclic Loading Tests of Masonry Single Piers, Volume 1—Height to Width Ratio of 2," Report No. UCB/EERC-78/27, University of California, Berkeley, 1978.
5. Hidalgo, P.A., Mayes, R.L., McNiven, H.D. and Clough, R.W., "Cyclic Loading Tests of Masonry Single Piers, Volume 3—Height to Width Ratio of 0.5," Report No. UCB/EERC-79/12, University of California, Berkeley, 1979.
6. Hidalgo, P.A., Mayes, R.L., McNiven, H.D. and Clough, R.W., "Seismic Behavior of Concrete Block Masonry Piers," Proceedings of the Third Canadian Conference on Earthquake Egineering, Montreal, Canada, 1979.
7. Mayes, R.L., Omote, Y. and Clough, R.W., "Cyclic Shear Tests of Masonry Piers, Volume 1—Test Results," EERC Report No. 76-8, University of California, Berkeley, 1976.
8. Mayes, R.L., Omote, Y. and Clough, R.W., "Cyclic Shear Tests on Masonry Piers, Volume 2—Analysis of Test Results," Report No. EERC 76-16, University of California, Berkeley, 1976.
9. Meli, R., "Behaviour of Masonry Walls under Lateral Loads," Proceedings on the Fifth World Conference on Earthquake Engineering, Rome, 1973.
10. Priestley, M.J.N. and Bridgeman, D.O., "Seismic Resistance of Brick Masonry Walls," Bulletin of the New Zealand National Society for Earthquake Engineering, Vol. 7, No. 4, 1974.
11. Priestley, M.J.N., "Seismic Resistance of Reinforced Concrete Masonry Shear Walls with High Steel Percentages," Bulletin of the New Zealand National Society for Earthquake Engineering, Vol. 10, No. 1, 1977.
12. Scrivener, J.C., "Concrete Masonry Wall Panel Tests with Predominant Flexural Effect," New Zealand Concrete Construction, 1966.
13. Williams, D.W., "Seismic Behavior of Reinforced Masonry Shear Walls," Ph.D. Thesis, University of Canterbury, Christchurch, New Zealand, 1971.

TABLE 1—General Test Results

Gross Cross Sections: HCBR-21 = 310 in^2, HCBR-11 = 354 in^2, HCBR-12 = 575 in^2, Net Cross Sections: HCBR-21 = 171 in^2
CBRC-21 = 420 in^2, CBRC-11 = 480 in^2, CBRC-12 = 780 in^2 HCBR-11 = 189 in^2

Specimen	Grouting Full (F) Partial (P) Solid (S)	Vertical Reinforcement		Horizontal Reinforcement				Ratio Of Total Area Of Steel To Gross Area Of Wall $p_v + p_h$	Average Ultimate Shear		Peak Ultimate Shear		Axial Compression At Ultimate		Shear Crack Strength*	Compressive Stress At Shear Crack*
		No. Bars	$p_v = \frac{A_{vs}}{A_g}$	No. Bars	Yield Strength (ksi)	$p_h = \frac{A_{hs}}{A_g}$	$A_{hs} f_y$ (kip)		Force (kip)	Stress* (psi)	Force (kip)	Stress* (psi)	Force (kip)	Stress* (psi)	(psi)	(psi)
HCBR-21-1	F	No	--	No	---	--	--	---	75.4	244	82.6	267	179.5	580	267	580
-2	F	2#8	0.0051	No	---	--	--	0.0051	63.7	206	73.7	238	113.9	368	238	368
-3	P	2#8	0.0051	No	---	--	--	0.0051	27.1	159	31.0	181	33.0	193	181	193
-4	F	2#8	0.0051	2#5	49.7	0.0020	30.8	0.0071	84.6	273	95.4	308	128.6	415	308	415
-5	P	2#8	0.0051	2#5	49.7	0.0020	30.8	0.0071	47.6	279	51.8	303	53.6	314	303	314
-6	F	2#8	0.0051	3#5	49.7	0.0030	46.2	0.0081	98.2	317	106.3	343	152.4	492	343	492
-7	P	2#8	0.0051	3#5	49.7	0.0030	46.2	0.0081	47.5	278	51.9	304	52.3	306	304	306
-8	F	2#8	0.0051	4#5	49.7	0.0040	61.6	0.0091	99.3	321	107.2	346	150.2	485	346	485
-9	F	2#8	0.0051	5#5	49.7	0.0050	77.0	0.0101	95.1	307	107.9	348	147.5	476	348	476
HCBR-11-1	F	No	--	No	---	--	--	---	90.1	255	98.5	278	116.1	328	278	328
-2	P	No	--	No	---	--	--	---	---	---	26.6	141	76.5	405	141	405
-3	F	2#5	0.0018	No	---	--	--	0.0018	94.4	267	98.9	279	52.3	148	279	148
-4	F	2#5	0.0018	1#5	70.0	0.0009	21.7	0.0026	119.3	337	124.8	353	114.3	323	353	323
-5	P	2#5	0.0018	1#5	70.0	0.0009	21.7	0.0026	45.4	240	52.4	278	53.7	284	278	284
-6	F	2#5	0.0018	5#5	64.2	0.0044	99.5	0.0061	116.2	328	122.4	346	61.9	175	346	175
-7	F	2#5	0.0018	5#5	72.6	0.0044	112.5	0.0061	94.6	267	99.2	280	85.3	241	280	241
-8	F	2#8	0.0045	No	---	--	--	0.0045	80.4	227	85.6	242	43.4	123	242	123
-9	P	2#8	0.0045	No	---	--	--	0.0045	43.0	228	49.1	260	37.3	198	260	198
-10	F	2#8	0.0045	2#5	68.7	0.0018	42.6	0.0062	101.6	287	104.8	296	54.2	153	296	153
-11	P	2#8	0.0045	2#5	68.7	0.0018	42.6	0.0062	46.0	244	51.9	275	26.7	141	275	141
-12	F	2#8	0.0045	5#6	73.9	0.0062	162.6	0.0107	94.3	266	97.2	275	85.0	240	275	240
-13	F	2#8	0.0045	5#6	74.7	0.0062	164.3	0.0107	113.3	320	116.3	329	110.6	312	329	312
HCBR-12-1	F	3#7	0.0031	No	---	--	--	0.0031	208.7	363	220.8	384	101.2	176	--	--
-2	F	3#7	0.0031	1#6	67.3	0.0008	29.6	0.0039	182.7	318	191.0	332	86.0	149	319	125
-3	F	3#7	0.0031	2#6	67.3	0.0015	59.2	0.0047	211.8	368	220.8	384	114.1	198	351	150
-4	F	3#7	0.0031	3#6	67.3	0.0023	88.8	0.0054	245.8	427	255.3	444	142.4	248	356	143
-5	F	3#7	0.0031	4#6	67.3	0.0031	118.4	0.0062	223.8	389	232.7	404	100.7	175	394	154
-6	F	3#7	0.0031	5#7	80.3	0.0052	240.9	0.0083	251.4	437	259.0	450	128.0	223	392	153
CBRC-21-1	S	No	--	No	---	--	--	---	92.7	221	100.3	239	221.7	528	--	--
-2	S	2#8	0.0038	No	---	--	--	0.0038	114.2	272	123.8	295	200.5	477	295	477
-3	S	2#8	0.0038	2#5	49.7	0.0015	30.8	0.0052	106.0	252	110.8	264	192.5	458	264	458
-4	S	2#8	0.0038	3#5	49.7	0.0022	46.2	0.0060	104.2	248	112.3	267	175.2	417	267	417
-5	S	2#8	0.0038	5#5	49.7	0.0037	77.0	0.0075	105.0	250	110.0	262	158.5	377	262	377
CBRC-11-1	S	No	--	No	---	--	--	---	114.9	239	118.6	247	141.9	296	247	296
-2	S	2#5	0.0013	No	---	--	--	0.0013	106.0	221	117.0	244	92.7	193	244	193
-3	S	2#5	0.0013	1#5	68.3	0.0006	21.2	0.0019	106.7	222	114.5	239	89.5	186	239	186
-4	S	2#5	0.0013	5#5	68.3	0.0032	105.9	0.0045	124.4	259	128.6	268	132.5	276	268	276
-5	S	2#8	0.0033	No	---	--	--	0.0033	102.0	213	104.3	217	76.4	159	217	159
-6	S	2#8	0.0033	2#5	73.9	0.0013	45.8	0.0046	128.3	267	130.4	272	100.3	209	272	209
-7	S	2#8	0.0033	5#6	74.7	0.0046	164.3	0.0079	115.7	241	123.3	257	80.9	169	257	169
CBRC-12-1	S	3#7	0.0023	No	---	--	--	0.0023	190.4	244	197.2	253	83.9	108	253	108
-2	S	3#7	0.0023	1#6	67.3	0.0006	29.6	0.0029	186.3	239	194.8	250	98.9	127	250	127
-3	S	3#7	0.0023	2#6	67.3	0.0011	59.2	0.0034	207.9	267	217.3	279	117.1	150	275	138
-4	S	3#7	0.0023	3#6	67.3	0.0017	88.8	0.0040	227.1	291	235.0	301	96.1	123	--	--
-5	S	3#7	0.0023	4#6	67.3	0.0023	118.4	0.0046	183.0	235	192.3	247	109.8	141	231	116
-6	S	3#7	0.0023	5#7	80.3	0.0038	240.9	0.0062	207.3	266	216.1	277	110.7	142	240	94

* Partially grouted pier stresses computed using net areas.

TABLE 2—Prediction of Shear Crack Strength for Fully Grouted Piers

Specimen	Vertical Steel Reinforcement (%)	Horizontal Steel Reinforcement (%)	Prism Compressive Strength f'_m (psi)	Square Panel Crit.Tensile Strength σ^o_{tcr} (psi)	Pier Shear Crack Strength τ_s (psi)	Pier Axial Stress at Shear Crack σ_c (psi)	Pier Critical Tensile Strength σ_{tcr}	$\frac{\sigma_{tcr}}{\sigma^o_{tcr}}$	$\frac{\tau_s}{\sqrt{f'_m}}$
HCBR-21-1	--	--	4502	375	267	-580	204	0.54	3.98
-2	0.51	--	4502	375	238	-368	218	0.58	3.55
-4	0.51	0.20	4502	375	308	-415	299	0.80	4.59
-6	0.51	0.30	4502	375	343	-492	325	0.87	5.11
-8	0.51	0.40	4502	375	346	-485	331	0.88	5.16
-9	0.51	0.50	4502	375	348	-476	336	0.90	5.19
HCBR-11-1	--	--	2535	282	278	-328	284	1.01	5.52
-3	0.18	--	2535	282	279	-148	352	1.25	5.54
-4	0.18	0.09	2722	363	353	-323	391	1.08	6.77
-6	0.18	0.44	2722	336	346	-175	438	1.30	6.63
-7	0.18	0.44	2535	282	280	-241	317	1.12	5.56
-8	0.45	--	2866	293	242	-123	307	1.05	4.52
-10	0.45	0.18	2722	363	296	-153	374	1.03	5.67
-12	0.45	0.62	2535	282	275	-240	309	1.10	5.46
-13	0.45	0.62	2722	363	329	-312	361	0.99	6.31
HCBR-12-2	0.31	0.08	2838	--	319	-125	420	--	5.99
-3	0.31	0.15	2838	--	351	-150	457	--	6.59
-4	0.31	0.23	2838	--	356	-143	467	--	6.68
-5	0.31	0.31	2838	--	394	-154	519	--	7.40
-6	0.31	0.52	2838	--	392	-153	516	--	7.36
CBRC-21-2	0.38	--	3315	284	295	-477	264	0.93	5.12
-3	0.38	0.15	3315	284	264	-458	228	0.80	4.59
-4	0.38	0.22	3315	284	267	-417	244	0.86	4.64
-5	0.38	0.37	3315	284	262	-377	247	0.87	4.55
CBRC-11-1	--	--	2507	205	247	-296	251	1.22	4.93
-2	0.13	--	2507	205	244	-193	282	1.38	4.87
-3	0.13	0.06	2507	205	239	-186	276	1.35	4.77
-4	0.13	0.32	2507	220	268	-276	287	1.30	5.35
-5	0.33	--	2507	205	217	-159	256	1.25	4.33
-6	0.33	0.13	2507	220	272	-209	316	1.44	5.43
-7	0.33	0.46	2507	220	257	-169	310	1.41	5.13
CBRC-12-1	0.23	--	2876	269	253	-108	329	1.22	4.72
-2	0.23	0.06	2876	269	250	-127	316	1.17	4.66
-3	0.23	0.11	2876	269	275	-138	349	1.30	5.13
-5	0.23	0.23	2876	269	231	-116	293	1.09	4.31
-6	0.23	0.38	2876	269	240	- 94	316	1.17	4.48

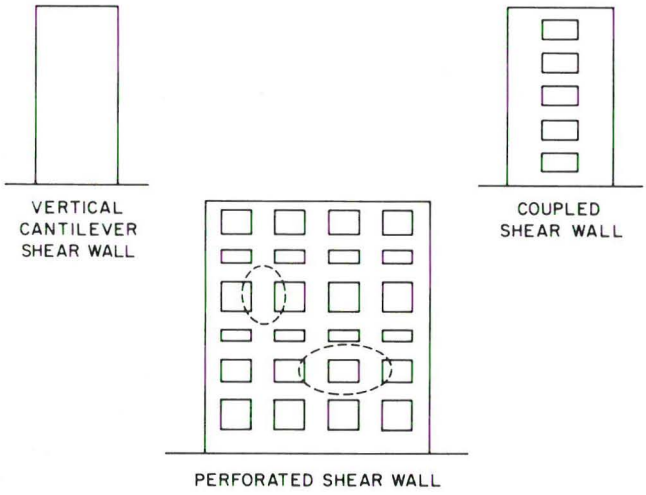

Figure 1. Typical Shear Walls

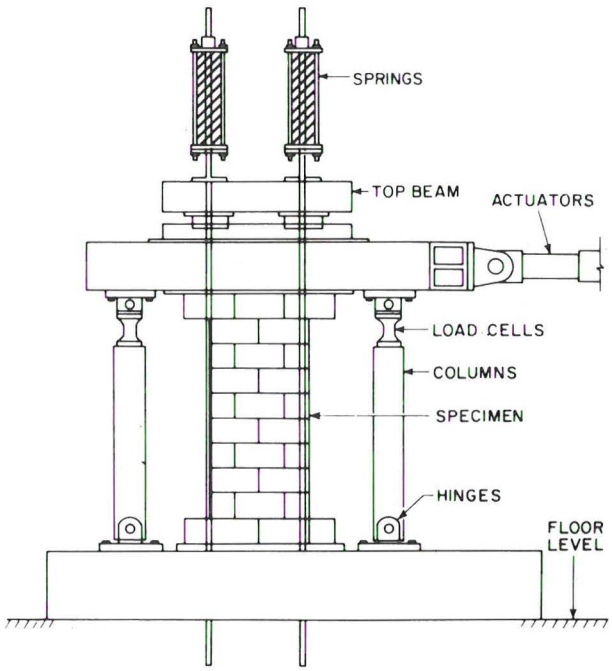

Figure 2. Single Pier Test Setup

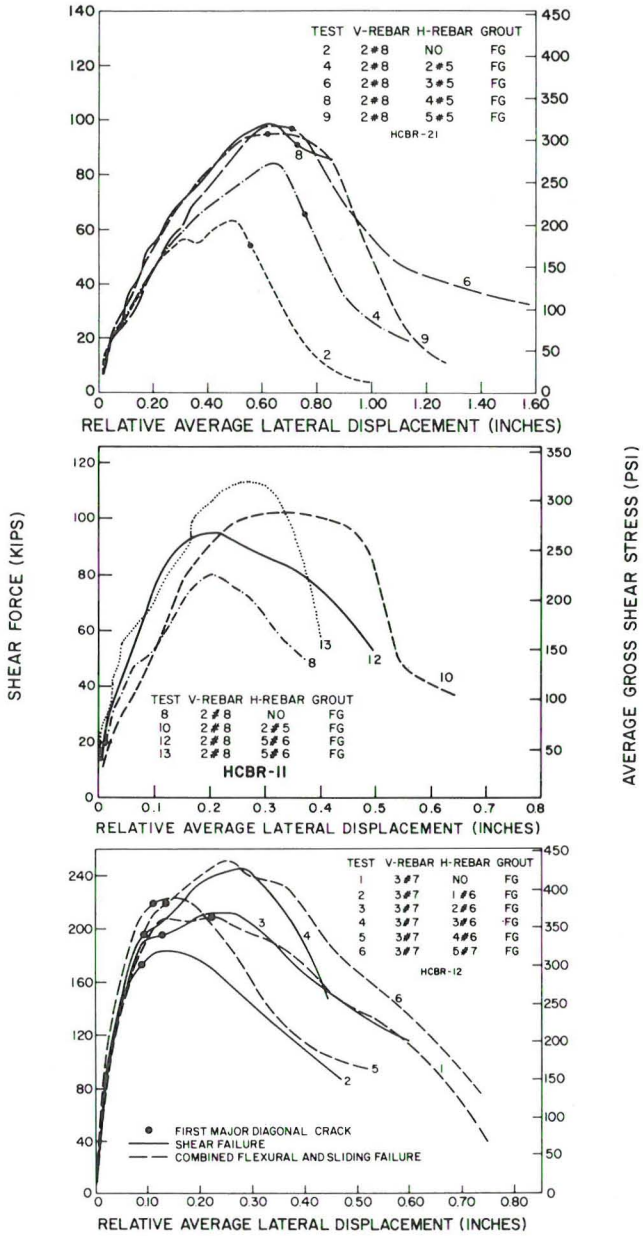

Figure 3. Effect of Horizontal Reinforcement on Hysteresis Envelope (HCBR Piers)

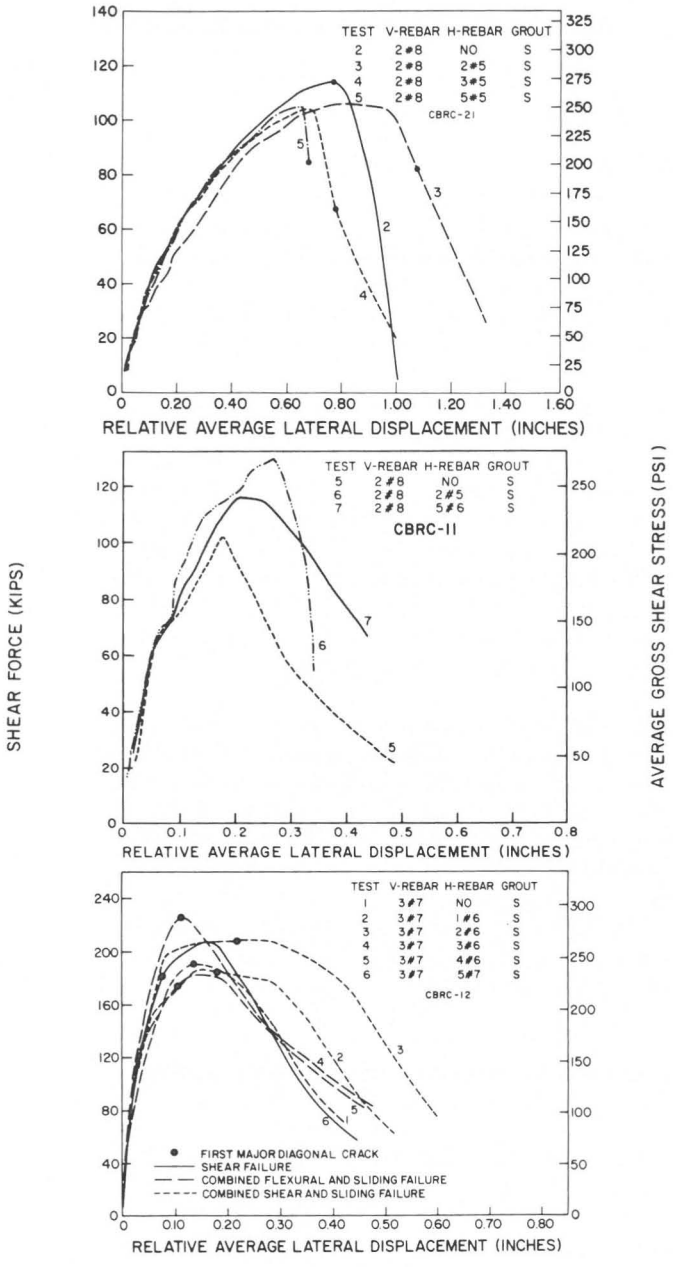

Figure 4. Effect of Horizontal Reinforcement on Hysteresis Envelope (CBRC Piers)

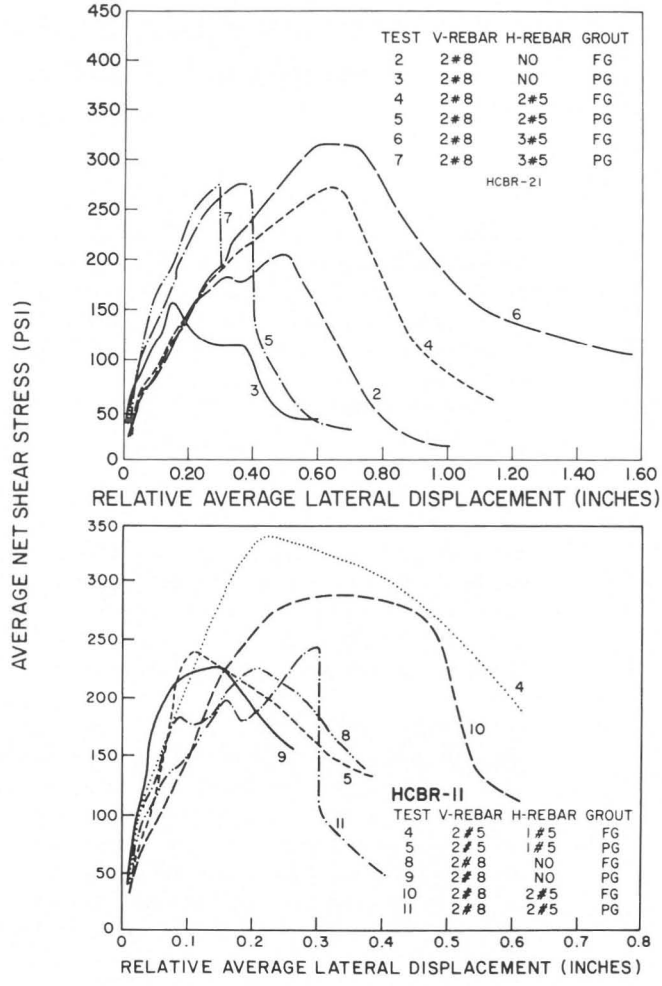

Figure 5. Effect of Partial Grouting on Hysteresis Envelope (HCBR Piers)